Hydro-climatology: Variability and change (Proceedings of symposium JH02 held during IUGG2011 in Melbourne, Australia, July 2011) (IAHS Publ. 344, 2011).

69

Statistical downscaling of daily rainfall for southeastern Australia

GUOBIN FU & STEPHEN P. CHARLES

CSIRO Water for a Healthy Country Flagship and CSIRO Land and Water, Australia
guobin.fu@csiro.au

Abstract An ensemble of stochastic daily rainfall projections has been generated for 30 stations across southeastern Australia using the downscaling Nonhomogeneous Hidden Markov Model (NHMM), which was driven by atmospheric predictors from four climate models for three IPCC emissions scenarios (A1B, A2, B1) and for two periods (2046–2065 and 2081–2100). The results indicate that the annual rainfall is projected to decrease for both periods for all scenarios and climate models, with the exception of a slight increase for one GCM for the A2 scenario in 2081–2100. However, there is a seasonal difference: two downscaled GCMs consistently project a decline of summer rainfall, and two an increase of summer rainfall. In contrast, all four downscaled GCMs show a decrease of winter rainfall. Since winter rainfall accounts for two-thirds of the annual rainfall and produces the majority of streamflow for this region, this decrease in winter rainfall would cause additional water availability concerns in the southern Murray-Darling Basin, given that water shortage is already a critical problem in the region. In addition, the annual maximum daily rainfall is projected to intensify in the future, particularly by the end of century; the maximum length of consecutive dry days is projected to increase and, correspondingly, the maximum length of consecutive wet days is projected to decrease. These changes in daily sequencing, combined with fewer events of reduced amount, would lead to drier catchment soil profiles and further reduce runoff potential, and hence also have streamflow and water availability implications.

Key words Murray-Darling Basin; Nonhomogeneous Hidden Markov Model (NHMM); southeastern Australia; statistical downscaling; climate change

INTRODUCTION

Research in the South Eastern Australian Climate Initiative (SEACI) commenced in 2006 to investigate the causes, impacts and prediction of climate variability and change in southeastern Australia (CSIRO, 2010). The SEACI study area covers all of Victoria, southern South Australia (including the agricultural areas of the Eyre Peninsula), and the Murray-Darling Basin (MDB). The MDB is Australia's most important agricultural region accounting for 40% of the gross value of agricultural production (Pigram, 2000) and 70% of all water used for irrigated agriculture in Australia. Precipitation and streamflow have experienced a significant decreasing trend in recent years, which is of immense concern to MDB water managers and irrigators (Cai & Cowan, 2008; Potter *et al.*, 2010). Therefore, future climate, particularly rainfall, is of utmost interest to resource management, agriculture and water-users in the region (Yu *et al.*, 2010).

The present generation of global and regional climate models are restricted in their usefulness for many sub-grid scale applications, including hydrology and water resources, due to their coarse spatial resolution. Downscaling attempts to resolve the scale discrepancy between climate change scenarios and the resolution required for hydrological and other impact assessment. It is based on the assumption that large-scale weather exhibits a strong influence on local-scale weather (Maraun *et al.*, 2010). Two approaches to downscaling exist. *Dynamical downscaling* nests a regional climate model (RCM) into the GCM to represent the atmospheric physics with a higher grid box resolution within a limited area of interest. *Statistical downscaling* establishes statistical links between large-scale weather circulation characteristics (such as mean sea level pressure or geopotential height) and observed local-scale weather (Maraun *et al.*, 2010).

The objectives of this study are to generate an ensemble of stochastic daily rainfall projections for 30 stations across southeastern Australia using the downscaling Nonhomogeneous Hidden Markov Model (NHMM), driven by atmospheric predictors from four climate models (CCAM, GFDL, Mk35 and MRI) for three IPCC emissions scenarios (A1B, A2, B1) and for two periods (2046–2065 and 2081–2100), and to assess projected changes in hydrologically relevant rainfall characteristics such as annual rainfall, seasonal rainfall, maximum, 99th, 95th and 90th percentile daily rainfall, as well as frequencies and maximum consecutive statistics of dry and wet days.

DATA AND METHODS

Data sets

There are three types of daily data required for statistical downscaling applications (Frost *et al.*, 2011): (a) historical rainfall data at meteorological stations; (b) large spatial-scale reanalysis predictors used with (a) for calibration and verification of the statistical downscaling model; and (c) GCM predictors interpolated to the same spatial scale as the reanalysis data, which for given scenarios into the future are used as the predictors to produce downscaled rainfall projections.

The 30 daily rainfall stations chosen for this study are located in the southern MDB in south-eastern Australia, between 142–150°E longitude and 33.5–38°S latitude. The sites chosen range from high altitude eastern regions (snow in winter season) to semi-arid sites in the west, with a range of climatological influences affecting rainfall (Chiew *et al.*, 2010; Frost *et al.*, 2011).

NCEP/NCAR Reanalysis (NNR) data, from 1961 to the present (Kalnay *et al.*, 1996), are used in the statistical downscaling model calibration. Many reanalysis variables are generated on a 2.5° by 2.5° latitude–longitude grid including sea level pressure, temperature and specific humidity at several levels in the atmosphere. Predictors are selected from a 6×5 grid domain of the 2.5° by 2.5° latitude–longitude grid centred on the chosen rainfall sites (for more details see Frost *et al.*, 2011).

Predictor data were also extracted from four GCMs: (a) CSIRO Mk3.5; (b) CCAM (atmosphere far field nudged and SSTs from CSIRO Mk3.0); (c) GFDL-CM2.0; and (d) MRI-CGM2.3.2a (as described at the website of the Program for Climate Model Diagnosis and Intercomparison (PCMDI) http://www-pcmdi.llnl.gov/). These were selected based on their current-day reproduction of the predictor fields required by the NHMM stochastic downscaling model as described in Charles & Fu (2008).

IPCC scenarios A1B, A2 and B1 are used in this paper. They were chosen due to data availability, however they do not represent the full range of possible climate change. The detailed description of these scenarios can be found at PCMDI website and IPCC reports (IPCC, 2007).

NHMM Model

The Nonhomogeneous Hidden Markov Model (NHMM) of Hughes *et al.* (1999) was selected to downscale atmospheric predictors to multi-site daily precipitation occurrence; then conditional multiple linear regression was selected to simulate multi-site daily precipitation amounts (Charles *et al.*, 1999). Previously the NHMM has been found suitable when applied to southwest Western Australia for historical (Hughes *et al.*, 1999; Charles *et al.*, 1999, 2004) and climate change studies (Bates *et al.*, 1998).

The NHMM models multi-site patterns of daily precipitation occurrence as a finite number of "hidden" (i.e. unobserved) weather states. The temporal evolution of these daily states is modelled as a first-order Markov process with state-to-state transition probabilities conditioned on a small number of synoptic-scale atmospheric predictors, such as sea-level pressure, geopotential heights, and measures of atmospheric moisture. Detailed information on the NHMM, including its mathematical parameterisations, estimation algorithms and assumptions can be found in Hughes *et al.* (1999) and Charles *et al.* (1999).

The NHMM was calibrated on an approximately half year basis, with summer defined as November–March and winter as April–October. The summer model has six weather states with three predictors: MSLP (mean sea level pressure), DTD700 (dew point temperature depression at 700 hPa, i.e. the difference between air and dew point temperature), and east–west GPH500 (geopotential height at 500 hPa) gradient. The winter model has five weather states and four predictors: north–south MSLP gradient, DTD700, DTD850, and north–south GPH700 gradient. Prior to their use in NHMM calibration, the atmospheric predictors extracted from NNR were converted to anomalies, i.e. "centred", by subtracting their calibration period means (Hughes *et al.*, 1999).

RESULTS AND DISCUSSION

Changes in weather state frequencies

The changes in NHMM downscaled weather state sequences are driven by the changes in atmospheric predictors projected by the GCM scenarios. The projected multi-site daily rainfall series are conditional on these weather state sequence changes, and thus the predictor changes. Table 1 summarises the five winter weather states, their calibration period frequencies and associated spatial rainfall patterns.

Table 1 Summary of winter weather state patterns.

State	Freq.	Description
1	0.48	Rainfall: dry everywhere Synoptics: high pressure centred over region; dry continental air
2	0.12	Rainfall: wet everywhere Synoptics: low pressure trough; moist southerly maritime airflow
3	0.10	Rainfall: moderately wet everywhere Synoptics: weak low pressure trough; moist system over region
4	0.18	Rainfall: wet in the south predominantly Synoptics: weak low pressure trough; moist southerly maritime airflow
5	0.12	Rainfall: wet everywhere, moderate in northwest Synoptics: low pressure trough further east than in State 2; moist southerly maritime airflow

Table 2 summarises the projected winter weather state frequency changes from downscaling the Mk3.5 projections (as an example, summer season and other GCM results are omitted due to space). The first number in each cell is the mean probability of occurrence (i.e. frequency) of the weather state for the given downscaled scenario. The second number, in brackets, is the number of "standard errors" between this probability and the baseline 20th century downscaled weather state probability (1961–2000). It is thus a measure of the relative significance of the projected change in weather state frequency.

Table 2 Winter Mk3.5 downscaled weather state mean frequencies (and standard errors, in brackets, relative to current climate).

State	Current	A1B mid*	A1B end	A2 mid	A2 end	B1 mid	B1 end
1	0.44	0.512 (3.4)	0.55 (5.3)	0.50 (2.6)	0.56 (6.1)	0.49 (2.4)	0.51 (3.9)
2	0.12	0.09 (2.8)	0.07 (5.0)	0.09 (2.1)	0.06 (5.7)	0.09 (2.6)	0.09 (2.9)
3	0.10	0.08 (2.5)	0.07 (4.2)	0.08 (2.1)	0.07 (4.5)	0.09 (1.5)	0.08 (2.6)
4	0.21	0.20 (0.6)	0.20 (0.4)	0.21 (1.1)	0.20(0.8)	0.21 (0.2)	0.21 (0.2)
5	0.14	0.12 (2.6)	0.11 (3.5)	0.11(3.1)	0.11 (4.1)	0.13 (1.5)	0.11(3.6)

* "mid" refers to the 2046–2065 period; "end" refers to the 2081–2100 period.

There is strong consistency in the direction of the state changes across virtually all the scenarios and periods. The dry State 1 increases in frequency for all scenarios and periods for both summer (not shown) and winter and the wet State 2, likewise, decreases. There is also a consistent response in the magnitude of the state changes to the different emissions scenarios by the end of the century, corresponding to the relative strength of each scenario.

Changes in annual and seasonal mean rainfall

The downscaled projections for annual rainfall, averaged across the 30 stations, indicate a decrease for both 2046–2065 and 2081–2100 periods for all scenarios and climate models (Fig. 1), except for a slightly increase for CCAM for the A2 scenario in 2081–2100. Note, CCAM results were not available for the B1 scenario. Two climate models (GFDL and Mk3.5) consistently project a decline of summer (Nov–Mar) rainfall, and two (CCAM and MRI) indicate an increase of summer

rainfall (Fig. 2). This is interesting considering that the CCAM model is nudged by the Mk3.0 atmosphere and uses the Mk3.0 SSTs as the ocean boundary condition. In contrast, all four downscaled climate models show a decrease of winter (Apr–Oct) rainfall (Fig. 2). Since winter rainfall accounts for two-thirds of the annual rainfall and produces the majority of streamflow for this region, this decrease would cause additional water availability concerns in the southern Murray-Darling Basin, given that water shortage is already a critical problem in the region.
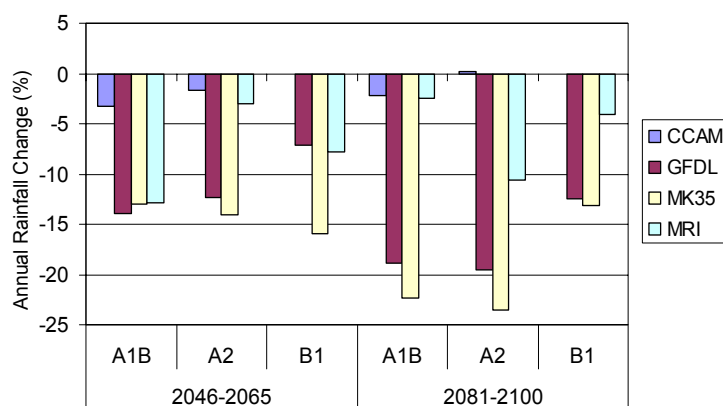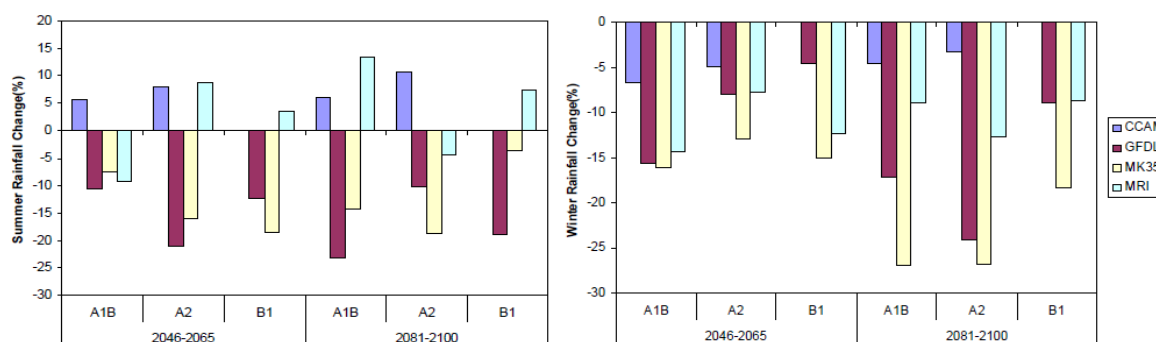

Fig. 1 Annual rainfall change (%).

Fig. 2 Summer and winter seasonal rainfall change (%).

Changes in extreme rainfall

The annual daily maximum rainfall is projected to intensify in the future, particularly by the end of the century (Fig. 3). This implies the potential for an increase in the probability and magnitude of intense floods in the study region (Fu *et al.*, 2010). The daily 99th percentile rainfall does not have as significant a change as the daily maximum rainfall. The changes are smaller than those of daily maximum rainfall, with more climate models and scenarios indicating a decrease (not shown). The daily 95th and 90th percentile rainfall values, in contrast, are projected to decrease in the future, especially for the 2081–2100 period (Fig. 3). The decrease in mean and increase in daily maximum rainfall is consistent with the recent literature (IPCC, 2007, and references therein).

Changes in dry/wet day frequencies

The number of dry days is projected to increase (Fig. 4) and accordingly wet days decrease (Fig. 4) consistently across all climate models and emission scenarios. This is consistent with analysis of GCM projections by Pitman & Perkins (2008). Together with the projected decrease in the annual rainfall this would decrease runoff and streamflow, and therefore suggests increasing water availability problems for the region.
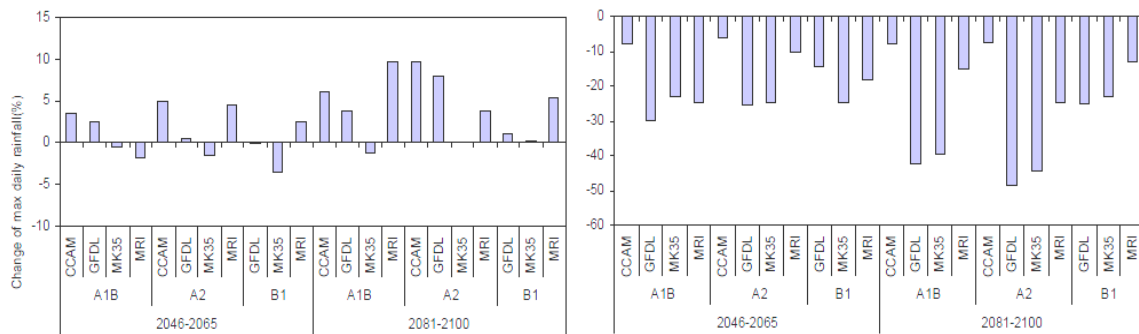
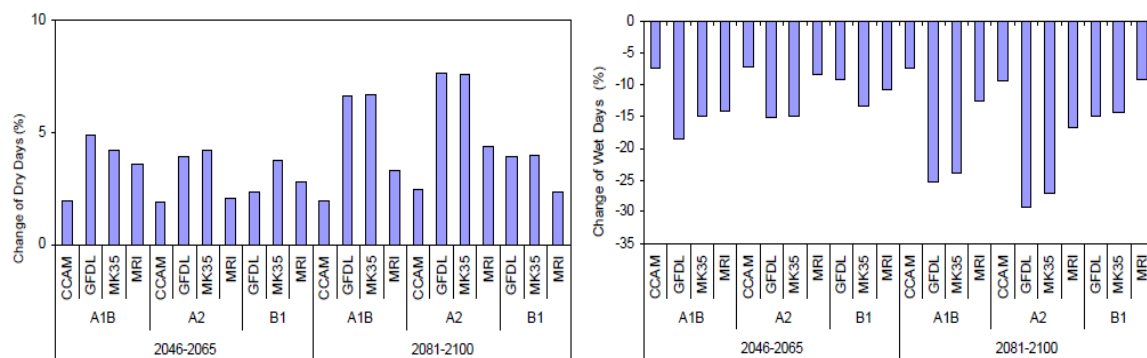**Fig. 3** Changes in annual daily maximum rainfall and daily 90th percentile rainfall (%).

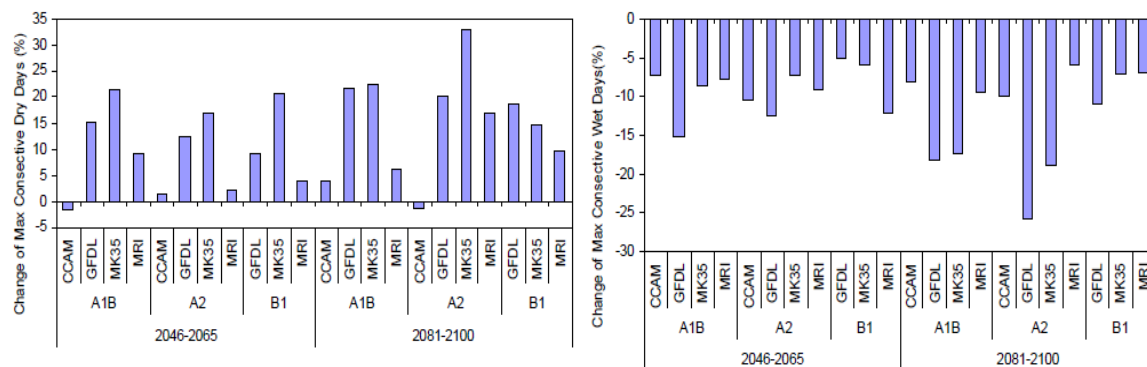**Fig. 4** Changes in dry (<1.0 mm) and wet (>=1.0 mm) days (%).

Fig. 5 Changes of maximum consecutive dry/wet days (%).

Changes in maximum consecutive dry/wet days

The maximum length of consecutive dry days is also projected to increase (Fig. 5). This change would dry out catchments, leading to reduced runoff and streamflow, with water availability implications. Correspondingly, there is a consistent projection for the maximum length of consecutive wet days to decrease (Fig. 5). These changes in daily sequencing, combined with fewer events and reduced amounts, would lead to drier catchment soil profiles and therefore further reduce runoff potential.

CONCLUSIONS

Stochastically downscaled multi-site daily rainfall projections were assessed for changes to hydrologically relevant metrics: annual, summer (Nov–Mar) and winter (Apr–Oct) rainfall, daily

maximum rainfall, daily 90th, 95th and 99th percentile rainfall, the number of dry and wet days, and the number of consecutive dry and wet days. Overall the results across the four climate models and three emissions scenarios for two periods in the future show consistent changes.

The results project rainfall changes that would lead to more occurrences of low streamflow because of the combined effect of changes in frequency, magnitude and sequencing of rainfall events. There is consistency among the four GCMs and three emission scenarios in a projected decrease in annual/winter rainfall, increase in dry days and maximum consecutive dry days and decrease in wet days and maximum consecutive wet days. This would have implications for reduced water availability in the region (e.g. Chiew *et al*., 2010). However, the increase of annual daily maximum rainfall could imply a potential increased risk of flooding. Important caveats are that: (1) these results are based on using a small number of GCMs and emission scenarios and so do not account for the full range of potential climate change, and (2) only one downscaling method is used; however, Frost *et al*. (2011) found consistency among six downscaling methods, including the NHMM, for this station network.

REFERENCES

Bates, B. C., Charles, S. P. & Hughes, J. P. (1998) Stochastic downscaling of numerical climate model simulations. *Environ. Model. Softw.* **13**(3-4), 325–331.

Cai, W. & Cowan, T. (2008) Evidence of impacts from rising temperature on inflows to the Murray-Darling Basin. *Geophys. Res. Lett.* **35**, L07701, doi:10.1029/2008GL033390.

Charles, S. P.& Fu, G. B. (2008) Extraction of statistical downscaling predictors from GCM output and assessment of GCM performance at the regional scale. Project 2.1.2., SEACI End of Project Report, CSIRO Land and Water, Australia.

Charles, S. P., Bates, B. C. & Hughes J. P. (1999) A spatio-temporal model for downscaling precipitation occurrence and amounts. *J. Geophys. Res. – Atmospheres* **104**(D24), 31657–31669.

Charles, S. P., Bates, B. C., Smith, I. N. & Hughes, J. P. (2004). Statistical downscaling of daily precipitation from observed and modelled atmospheric fields. *Hydrol. Processes* **18**(8), 1373–1394

Chiew, F. H. S, Kirono, D. G. C., Kent, D. M., Frost, A. J., Charles, S. P., Timbal, B., Nguyen, K. C. & Fu, G. (2010) Comparison of runoff modelled using rainfall from different downscaling methods for historical and future climate. *J. Hydrol.* **387**, 10–23.

CSIRO (2010) Climate variability and change in south-eastern Australia: A synthesis of findings from Phase 1 of the South Eastern Australian Climate Initiative (SEACI), CSIRO, Australia, 31pp.

Frost, A. J., Charles, S. P., Timbal, B., Chiew, F. H. S., Mehrotra, R., Nguyen, K. C., Chandler, R. E., McGregor, J. L., Fu, G., Kirono, D. G. C., Fernandez, E. & Kent, D. M. (2011) A comparison of multi-site daily rainfall downscaling techniques under Australian conditions. *J. Hydrol.* (in review).

Fu, G. B., Viney, N. R., Charles, S. P. & Jianrong Liu (2010) Long-term temporal variation of extreme rainfall events in Australia: 1910–2006. *J. Hydromet.* **11**, 950–965.

Hughes, J. P., Guttorp, P. & Charles, S. P. (1999) A non-homogeneous hidden Markov model for precipitation occurrence. *J. Royal Stat. Soc., Series C–Applied* **48**(1), 15–30.

IPCC (2007) *Climate Change 2007: Synthesis Report*. Contribution of Working Groups I, II and III to the Fourth Assessment Report of the Intergovernmental Panel on Climate Change [Core Writing Team, R. K Pachauri & A. Reisinger (eds.)]. IPCC, Geneva, Switzerland, 104 pp.

Kalnay, E., Kanamistsu, M. *et al*. (1996) The NCEP/NCAR 40-Year Reanalysis Project. *Bull. Am. Met. Soc.* **77**(3), 437–471,

Maraun, D., *et al*. (2010) Precipitation downscaling under climate change: Recent developments to bridge the gap between dynamical models and the end user. *Rev. Geophys.* **48**, RG3003, doi:10.1029/2009RG000314.

Pigram, J. J. (2000) Towards upstream–downstream hydrosolidarity – Australia's Murray-Darling River Basin. *Water Int.* **25**, 222–226.

Pitman, A. J. & Perkins, S. E. (2008) Regional projections of future seasonal and annual changes in rainfall and temperature over Australia based on skill-selected AR4 models. *Earth Interactions* **12**, 1–50.

Potter N. J., Chiew, F. H. S. & Frost, A. J. (2010) An assessment of the severity of recent reductions in rainfall and runoff in the Murray-Darling Basin. *J. Hydrol.* **381**, 52–64.

Yu, J. J., Fu, G. B., Cai, W. & Cowan, T. (2010) Impacts of precipitation and temperature changes on annual streamflow in the Murray-Darling Basin. *Water Int.* **35**, 313–323.